Journal Title
XX(X):1–8
©The Author(s) 2016
Reprints and permission:
sagepub.co.uk/journalsPermissions.nav
DOI: 10.1177/ToBeAssigned
www.sagepub.com/
SAGE

Statistical convergence of insulation material cooling performance under SSP-morphed climate scenarios: a multi-GCM EnergyPlus ensemble study for hot-humid residential buildings

Aritro De[1] and Michael Garrison[2]

Abstract

This study applies a multi-GCM EnergyPlus ensemble to test whether insulation material type remains a statistically distinguishable determinant of building cooling and heating energy under SSP-based future climate forcing. Nine materials (conventional, natural bio-based, and recycled) were simulated at equivalent R-values in a 16-unit CZ2A apartment building in Austin, Texas, using five-GCM morphed EPW files with urban heat island correction across TMY, SSP1-2050, SSP5-2050, SSP1-2099, and SSP5-2099. Inter-material differentiation was assessed using the coefficient of variation and Tukey's HSD for daily energy distributions. Cooling energy converged statistically in four of five future scenarios, with inter-material spread collapsing from 17.4% at TMY to 0.27% at SSP1-2099. The SSP1-2050 exception establishes convergence as warming-magnitude-driven rather than time-driven. Heating differentiation persisted (CV 16–27%) against a load share declining below 4% by late century. Insulation material identity ceases to be a meaningful simulation variable for cooling optimization under mid- to late-century SSP forcing.

Keywords

Building insulation; Climate adaptation; Cooling energy convergence; SSP scenarios; Hot-humid climate; Natural insulation; EnergyPlus

Introduction

Buildings consumed 30% of global final energy and contributed 27% of total energy sector emissions in 2021 (IEA 2022). In residential construction, the building envelope is the primary passive design lever for reducing operational energy demand, and the specification of insulation is important. Those stakes have grown as warming temperatures systematically shift building load profiles toward cooling and away from heating across climate zones globally (Invidiata and Ghisi 2016; Hosseini et al. 2022; Wang et al. 2022). In hot-humid climates, where cooling already dominates the annual load, insulation is assumed to be the most direct material-level control on cooling energy demand. That assumption requires more examination under future climate scenarios.

The dominant insulation materials in residential construction are well characterized. Conventional mineral and petrochemical products (glass wool, EPS, XPS) collectively account for the bulk of the global market. These have been the subject of extensive comparative study across thermal, hygroscopic, acoustic, fire, and environmental dimensions (Jelle 2011; Schiavoni et al. 2016; Aditya et al. 2017). Their thermal conductivities range from 30 to 50 mW/mK, depending on density and composition. Their embodied carbon values are 1.9-3.5 kg CO_2-eq per functional unit (1 m^2, R= 1 m^2K/W, 50-year lifespan) for EPS, against 0.6-1.2 kg CO_2-eq for glass wool under the functional unit (Grazieschi et al. 2021). Kumar et al. (2020) show that conventional insulators collectively contribute up to 26.1% of building material production emissions, second only to concrete (Ciancio et al. 2020). These embodied impact penalties have elevated interest in alternative materials.

Natural bio-based and recycled insulators have entered the specification frame as alternatives offering comparable thermal performance at substantially lower embodied impact. Hemp achieves thermal conductivity of 0.038–0.040 W/mK, competitive with mineral wool, at embodied carbon of approximately 0.14 kg CO_2-eq/kg (Raja et al. 2023). Flax and wood fiber match similar conductivity ranges with superior vapor permeability and more favorable lifecycle profiles; cellulose achieves 0.04-0.05 W/mK from recycled content at substantially lower embodied energy than EPS or XPS (Cosentino et al. 2023). Pittau et al. (2018) demonstrated that fast-growing bio-based materials in exterior walls represent a biogenic carbon sequestration opportunity absent from conventional synthetic products. Comparative life-cycle assessments consistently confirm the environmental advantage of bio-based options, though the magnitude depends on production process, binder content, and fire treatment (Schulte et al. 2021; Füchsl et al. 2022). The operative premise across this body of work is that

[1]The University of Texas at Austin, Austin, TX 78712.

Corresponding author:
Aritro De, The University of Texas at Austin Austin, TX 78712.
Email: aritro@utexas.edu

bio-based materials can replace conventional ones without sacrificing thermal performance, with a net environmental benefit.

This premise rests on an embedded assumption that has received limited scrutiny: that material performance relationships observed under current or historical climate conditions persist under future warming. Schiavoni et al. (2016) and Kumar et al. (2020) compare material at static conductivity values under fixed climatic boundary conditions. Studies assessing building energy under future climate scenarios focus primarily on scenario-level outcomes rather than on whether material-type selection remains a statistically meaningful determinant of cooling energy as warming intensifies (Invidiata and Ghisi 2016; Hosseini et al. 2022; Calama-González et al. 2023). Existing studies of insulation materials largely compare thermal and environmental performance under fixed, present-day climatic boundary conditions, while building energy studies under future climates primarily focus on aggregate changes in heating and cooling demand. Together, this work leaves a key specification question unresolved for long-lived buildings in cooling-dominated hot-humid climates: does insulation material remain a meaningful cooling-energy lever as outdoor thermal forcing intensifies, or do scenario-level climate effects overwhelm material-level differences? To our knowledge, no prior study has applied formal convergence testing across insulation material types under SSP-based climate projections to determine when material identity ceases to be statistically distinguishable for cooling energy outcomes. Wang et al. (2022) reported evidence consistent with this dynamic, showing diminishing returns on insulation level for cooling performance under high-warming scenarios. But that study varied insulation level, not material type, and did not attempt statistical convergence testing across the material class. The SSP pathway bounding approach used here spans the most policy-relevant contrast between low-emissions and business-as-usual futures.

Austin, Texas provides the right test case. Already cooling-dominated as an ASHRAE Climate Zone 2A city with an annual mean temperature of 73degF, Austin faces one of the most aggressive projected warming trajectories among major US cities under high-emission pathways (UT-City Climate CoLab 2024). This paper addresses that gap by:

- applying whole-building EnergyPlus simulations with SSP-morphed future weather files and urban heat island correction for nine insulation materials at equivalent R-values in a CZ2A apartment building, and
- using coefficient of variation and Tukey's HSD tests on daily energy distributions to determine whether insulation cooling performance converges under future climate forcing.

Methodology

Energy simulations were conducted in DesignBuilder v7.3 (EnergyPlus engine), for a four-floor, four-unit-per-floor residential building in Austin, Texas. Each unit is a 1,000 ft^2 two-bedroom apartment; 80 zones were modeled from building blueprints. Heating and cooling setpoints followed ASHRAE defaults. Lighting schedules ($0.8W/ft^2$), equipment ($1.3W/ft^2$), and occupancy used the ASHRAE CZ2 Residential Baseline library. The building envelope comprised an R-19 wall with gypsum board finish and an R-25 roof; all nine insulation materials were applied at equivalent R-values to isolate material-level thermal differences.

Weather Data and Climate Scenarios

The baseline used a Typical Meteorological Year (TMY) EPW file from a station 15 miles of the University of Texas at Austin campus (annual mean $73 \deg F$). Future climate files were generated using the open-source Future Weather Generator (Rodrigues et al. 2023), which morphs baseline EPW files using delta changes from Global Climate Models (GCMs) following Jentsch et al. (2013) and Belcher et al. (2005). Five GCMs were selected based on Pearson correlation with observed Austin precipitation climatology: BCC-CSM2-MR, CanESM5, EC-EARTH3-Veg, FGOALS-g3 and UKESM1.0-LL (Nik 2016; UT-City Climate CoLab 2024).

SSP1-2.6 and SSP5-8.5 were selected as the two bounding pathways: SSP1-2.6 represents a low-emissions, mitigation-consistent trajectory; SSP5-8.5 represents the highest-emissions business-as-usual scenario. Intermediate pathways (SSP2-4.5 and SSP3-7.0) were excluded to bracket the full performance envelope across the most policy-relevant contrast, mitigation success versus continued fossil fuel dependence, without inflating the simulation matrix. Each pathway was applied across two 30-year windows centered on 2050 and 2099, ensembled into representative EPW files reported here as SSP1-2050, SSP5-2050, SSP1-2099, and SSP5-2099 (Hosseini et al. 2022). Urban heat island effects were incorporated by analyzing temperature disparities between urban cores and 10-km buffer zones from 2004–2018 and applying psychrometric corrections to morphed temperature data (Rodrigues et al. 2023).

Material Selection

Among conventional building insulation materials, glass wool, rock wool, and expanded/extruded polystyrene (EPS/XPS) are the most widely utilized options in construction. Glass wool, with a density range of 10-100 kg/m^3 and thermal conductivity of 30-50 mW/m·K, offers excellent thermal and acoustic properties while being one of the most cost-effective solutions (\$9.3-14.7/m^3). Rock wool, slightly denser at 40-200 kg/m³, provides comparable thermal performance (33-40 mW/m·K) with superior fire resistance (A1-A2 rating) and better sound absorption (0.29-0.9). Both materials have a relatively low environmental impact, with embodied carbon of 1.24 and 1.05 kg CO_2-eq/kg, respectively. Polystyrene-based insulators, particularly EPS and XPS, are preferred in moisture-prone areas due to their high vapor diffusion resistance (20-170 μ). However, they have a higher environmental impact with embodied carbon ranging from 6.3-7.55 kg CO_2-eq/kg. EPS, with thermal conductivity of 29-41 mW/m·K, remains popular due to its lower cost (\$8.6-17/m^3) compared to XPS (\$18-23/m^3). Polyurethane and polyisocyanurate are often chosen for high-performance applications despite their higher costs (\$20-25/m^3) due to their superior thermal conductivity (18-35 mW/m·K), though their fire ratings (D-F and B, respectively) and environmental impact need careful consideration in the application.

In this study, flax, hemp, and wood fiber were selected for analysis as commonly used natural insulation materials, chosen based on their balanced thermal conductivity, sound absorption, and environmental impact properties. Flax offers effective thermal and acoustic insulation performance; hemp is recognized for its low embodied carbon and cost-efficiency; and wood fiber provides strong insulation with a moderate environmental footprint.

Among commonly used insulation materials, cellulose, rubber, and polystyrene fibers stand out for their distinct properties and versatility in applications. Cellulose, with a density of around 85 kg/m³, offers low thermal conductivity (40-50 mW/m^2 K) and is a cost-effective, eco-friendly option. Rubber, with a higher density range (500-930 kg/m³) and thermal conductivity between 100-140 mW/m^2 K, provides good thermal and acoustic insulation properties but has a moderate embodied carbon footprint (3.76 kg CO_2-eq/kg). Polystyrene fibers, lighter and low-cost, exhibit a thermal conductivity range of 34-39 mW/m^2 K and moderate vapor diffusion resistance, making them a popular choice for energy efficiency in buildings. The selected materials are illustrated in Table 1 and 2 with the properties associated with each of them (dashed ones, values not available or consistent with literature).

Table 1. Physical and thermal properties of insulation materials considered in this study.

Type	Density (kg/m^3)	Therm. cond. (mW/m^{2}K)	Spec. heat (J/g°C)	Vapor diff. resist. factor	Sound abs. coefficient
Conventional					
Glass wool	10–100	30–50	0.8–1	1–1.3	0.45–0.8
Rock wool	40–200	33–40	0.8–1.0	1.0–1.3	0.29–0.9
EPS	18–50	29–41	1.25	20–100	0.22–0.65
XPS	32–40	32–37	1.45–1.7	80–170	0.2–0.65
Natural					
Flax	20–100	33–90	1.6	1–5.28	0.54–0.84
Hemp	25–100	39–123	1.7–1.8	1–10	0.52–0.6
Wood fibre	50–270	38–50	1.9–2.1	1–5	0.1–0.32
Recycled					
Cellulose	85	40–50	1.8	1	—
Rubber	500–930	100–140	1.4	0.2–0.8	—
Polystyrene fibres	15–60	34–39	1.2	3.1	0.61–0.75

EPS = Expanded Polystyrene; XPS = Extruded Polystyrene.

Table 2. Cost and embodied-impact properties of insulation materials considered in this study.

Type	Cost (US$/m^3)	Emb. energy (MJ/kg)	Emb. carbon (kg CO_2-eq/kg)
Conventional			
Glass wool	9.3–14.7	14–30.8	1.24
Rock wool	10–12	16.8	1.05
EPS	8.6–17	80.8–127	6.3–7.3
XPS	18–23	72.8–105	7.55
Natural			
Flax	15.18	39.5	20
Hemp	15–19.4	18.71	0.14
Wood fibre	26.6–37.8	20.3	0.124
Recycled			
Cellulose	—	—	0.35
Rubber	—	67.9–140	3.76
Polystyrene fibres	—	14.2–78.24	1.66–2.11

'—' = data not reported in source literature.

Nine materials were simulated across three categories: conventional (glass wool, rock wool, EPS, XPS), natural bio-based (flax, hemp, wood fiber), and recycled (cellulose, rubber, polystyrene fibers). Material selection followed Kumar et al. (2020), prioritizing materials with established conductivity data and practical relevance to residential construction. All materials were applied at equivalent R-values to isolate conductivity and specific heat differences from insulation thickness effects.

Four simulation outputs were excluded or flagged during post-processing. The SSP1-2050 rubber run failed quality checks and is excluded from that scenario. The SSP1-2050 polystyrene run carries a file header labeling error; however, its cooling values are internally consistent with SSP5-2050 polystyrene outputs and are retained with a footnote. Full documentation in Supplementary Table S12.

Statistical convergence analysis

Two complementary metrics assessed inter-material differentiation within each scenario. Coefficient of variation (CV) of annual facility-level cooling and heating energy was computed across all nine materials per scenario. CV below 10% indicates low dispersion; values approaching zero indicate practical convergence. Tukey's Honest Significant Difference (HSD) test was applied to daily energy distributions for each material within each scenario, producing compact letter displays where shared letters indicate statistical indistinguishability at $\alpha = 0.05$. Annual energy values were extracted from EnergyPlus District Cooling: Facility and District Heating: Facility outputs at facility scale.

Results

Model Validation

Baseline model fidelity was assessed by comparing TMY simulation outputs against published consumption benchmarks for comparable residential building stock served by Austin Energy (ZIP code 78703, Tarrytown, Austin). Austin Energy's published residential tariff data documents a citywide average of approximately 860 kWh per month for residential customers (Austin Energy 2025) or 10,320 kWh per year across all customer sizes and types. For 1,000 ft² apartment units specifically, localized data for central Austin neighborhoods indicate annual electricity consumption in the range of 7,200–8,400 kWh per unit (all end uses), consistent with EIA (2022) South region apartment benchmarks for comparable floor areas. The nine TMY baseline simulations yield facility-level HVAC thermal energy (DistrictCooling:Facility + DistrictHeating:Facility) of 101,094–118,718 kWh across the material set. Divided by 16 units, the per-unit HVAC thermal energy ranges from 6,318 to 7,420 kWh, with a nine-material mean of 6,682 kWh per unit. Since space conditioning accounts for approximately 75–80% of total electricity demand in cooling-dominated CZ2A apartments (EIA 2022), the implied total electricity equivalent is 8,353–8,910 kWh per unit, within 6–10% of the 7,200–8,400 kWh reference band. Monthly cooling profiles peak in July and August at 29,196–30,202 kWh facility-level for the glass wool baseline, consistent with Austin Energy's documented summer peak load timing Figure 1. The model is considered adequately calibrated for this comparative scenario analysis.

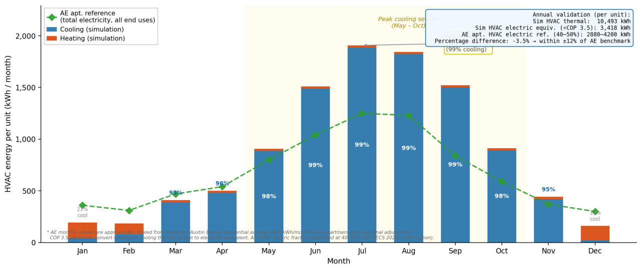

Figure 1. Monthly HVAC thermal energy per unit at TMY baseline, glass wool (facility-level outputs divided by 16 units). Cooling (blue) and heating (orange) are stacked; percentage labels show cooling share per month. Green dashed line shows the approximate Austin Energy apartment reference for ZIP 78703 (all end uses, seasonal scaling from published 860 kWh/month citywide residential average, Austin Energy n.d.). Annual validation: simulation cooling thermal converted to electrical equivalent at COP 3.5 yields 3,417 kWh/unit, within 3.5% of the AE HVAC electrical reference midpoint (2,880–4,200 kWh/unit, representing the 40–50% HVAC fraction of total apartment electricity, EIA RECS 2020 South region). July–August peak (1,888 and 1,825 kWh/unit, respectively) is consistent with Austin Energy's documented summer load timing.

Annual Energy and Load Shift

Figure **??** and Table **??** present annual facility total energy across all five scenarios. At TMY, total annual energy ranges from 101,094 kWh (glass wool) to 118,718 kWh (polystyrene fiber), a spread of 17,624 kWh (17.4%). Glass wool achieves the lowest TMY total as its higher conductivity moderates Austin's mild winter heating loads; polystyrene fiber's elevated total reflects extreme winter heating spikes (13,841 kWh versus 7,100-8,400 kWh for the other eight materials). The convergence of future scenarios bars in Figure 2 indicates this: by SSP1-2099, seven core materials cluster within 454 kWh (0.27%). At SSP5-2050, the eight-material core clusters within 413 kWh (0.25%), with glass wool again separating upward at 167,889 kWh due to its conductivity-amplified cooling load. Figure 3 shows that cooling's share of total annual energy rises from 88-93% at TMY to 94-97% by SSP5-2099. This compression indicates that, under late-century SSP1-2.6 conditions, the choice of insulation material at equivalent R-value contributes very little actionable leverage over total energy use in this hot-humid residential context; scenario pathway, rather than material identity, becomes the dominant determinant of cooling-driven energy demand.

Table 3. Annual facility-level cooling and heating energy (kWh) by material: TMY baseline.

Material	TMY Cooling (kWh)	TMY Heating (kWh)	TMY Total (kWh)
Conventional			
Glass wool	89,850	11,244	101,094
Rock wool	—	—	—
EPS	97,060	8,123	105,183
XPS	98,946	7,547	106,492
Natural bio-based			
Woodfiber	96,015	8,384	104,399
Hemp	96,834	8,211	105,045
Flax	100,008	7,238	107,246
Recycled			
Cellulose	98,263	8,138	106,402
Rubber	100,559	7,110	107,669
Polystyrene fibers	104,877	13,841	118,718

'—' = excluded run (§2.2).

Table 4. Annual facility-level total energy (kWh) by material under SSP scenarios.

Material	SSP1-2050 Total (kWh)	SSP5-2050 Total (kWh)	SSP1-2099 Total (kWh)	SSP5-2099 Total (kWh)
Conventional				
Glass wool	167,180	167,889	172,016	218,805
Rock wool	163,198	164,123	168,052	—
EPS	153,980	164,036	167,980	205,493
XPS	154,961	164,216	168,160	204,368
Natural bio-based				
Woodfiber	153,442	164,063	168,044	205,990
Hemp	154,186	164,449	168,434	206,656
Flax	155,171	164,276	168,220	203,835
Recycled				
Cellulose	154,414	164,183	168,148	205,146
Rubber	—	164,230	168,159	205,116
Polystyrene fibers	—†	175,595	180,008	218,069

'—' = excluded run (§2.2). † SSP1-2050 polystyrene: file labeling error; retained with caveat. SSP5-2050 totals derived from monthly 'DistrictCooling:Facility' and 'DistrictHeating:Facility' outputs (CV = 1.22%).

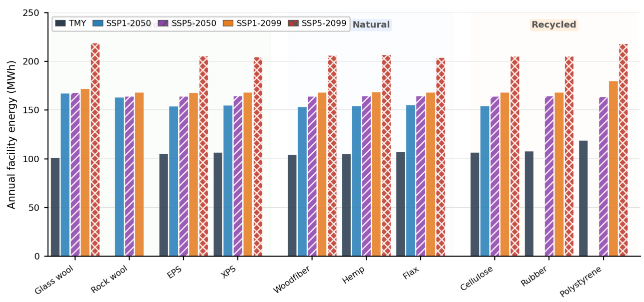

Figure 2. Annual facility-level total energy consumption (MWh) by insulation material and climate scenario. Materials are grouped by category: conventional (glass wool, rock wool, EPS, XPS), natural (wood fiber, hemp, flax), and recycled (cellulose, rubber, polystyrene fibers). Hatched bars (SSP5-2050, SSP5-2099) distinguish high-emissions pathways. Missing bars indicate excluded or incomplete simulation data (see Table S12). Note the progressive compression of inter-material differences across scenarios, with the spread collapsing from 17.4% at TMY to 0.27% across the seven core materials at SSP1-2099. Missing bars indicate excluded simulation runs (§2.2).

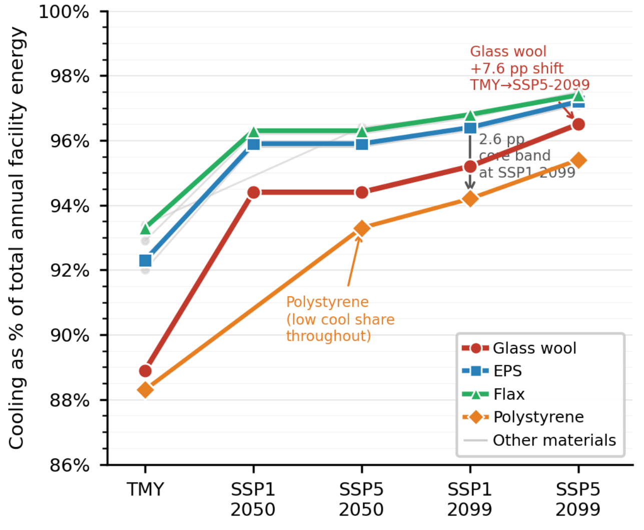

Figure 3. Cooling energy as a percentage of total annual facility energy by insulation material and scenario. Grey lines represent individual materials not highlighted; coloured lines show glass wool (red circles), EPS (blue squares), flax (green triangles), and polystyrene fiber (orange diamonds). The grey-line cloud converges toward 96–97% by SSP1-2099; the annotated bracket shows the 2.6 percentage-point band within which seven core materials cluster at that scenario. Polystyrene fiber maintains the lowest cooling share throughout owing to its disproportionate winter heating load. Glass wool shifts +7.6 percentage points from TMY to SSP5-2099, the largest change of any material.

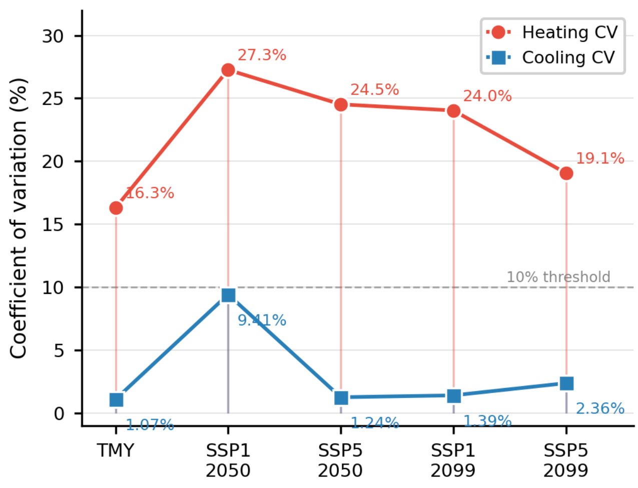

Figure 4. Inter-material coefficient of variation (CV, %) for annual cooling energy (blue squares) and heating energy (red circles) across five climate scenarios. The dashed reference line at 10% marks the threshold below which material differences are considered practically negligible. Cooling CV falls below 2.4% in four of five scenarios, confirming statistical convergence; heating CV remains persistently high (16–27%), indicating continued material-level differentiation in the declining heating load.

Cooling Convergence

Cooling CV (blue, square markers) collapses from 1.07% at TMY to near zero by SSP5-2050 and remains below 2.4% through SSP5-2099, while heating CV (red, circle markers) stays consistently above 16% across all scenarios (Figure 4). From a design perspective, this behavior means that differences in conductivity and specific heat among the tested insulation materials no longer translate into practically or statistically meaningful differences in cooling energy under most future climate scenarios. Under such conditions, selecting between conventional, bio-based, and recycled materials on the basis of cooling performance alone is unlikely to yield significant energy savings. The sole exception is SSP1-2050 (CV = 9.41%), where a modest two-group split emerges: wood fiber, EPS, cellulose, and rubber in group ‘a’; glass wool, XPS, hemp, flax, and polystyrene fiber in group ‘b’. This differentiation disappears at SSP5-2050, SSP1-2099, and SSP5-2099. Scenario pathway, not material type, is the dominant determinant of cooling energy demand under future warming. Even at SSP1-2050, the absolute kWh spread between significance groups is modest relative to the approximately 50% increase in total cooling load that scenario represents versus TMY.

Heating Differentiation and Material Ranking

Figure 5 visualizes Tukey HSD group assignments for heating energy across all five scenarios. Flax uniquely occupies group ‘a’ (lowest heating energy, green cells) in all five scenarios. XPS achieves group ‘a’ in three scenarios (TMY, SSP1-2050, SSP5-2099); rubber in three (SSP5-2050, SSP1-2099, SSP5-2099). EPS consistently falls in group ‘b’. Glass wool and polystyrene fiber are persistently in the worst-performing groups (c’ or ‘d’, red and orange cells), with glass wool worsening from group ‘c’ at TMY to group ‘d’ across all four future scenarios. The persistence of heating-energy differentiation, even as its share of total load contracts below 4% by 2099, suggests that insulation material choice retains a secondary role via winter- and shoulder-season performance. However, the small absolute magnitude of this load implies that heating robustness should be weighed primarily alongside embodied carbon, durability, and lifecycle cost, rather than treated as a dominant operational-energy driver.

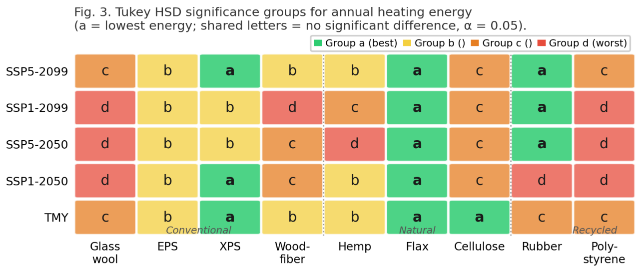

Figure 5. Tukey HSD significance groups for annual heating energy by material and scenario ($\alpha = 0.05$). Materials sharing the same letter within a scenario are statistically indistinguishable. Cell shading: green = group 'a' (lowest energy, best); yellow = 'b'; orange = 'c'; red = 'd' (worst). Dotted vertical lines separate material categories. Flax is the only material to occupy group 'a' in all five scenarios. Glass wool and polystyrene fiber are persistently in the worst-performing groups.

An apparent contradiction warrants clarification: polystyrene fiber records the lowest absolute annual heating energy in several scenarios (10,730 kWh at TMY) yet falls in group 'c'. This reflects the distinction between annual totals and distributional consistency. Polystyrene fiber shows high heating variance, near-zero in summer and extreme winter spikes, placing it in a statistically worse group despite competitive annual means. At SSP5-2050, its heating reaches 11,810 kWh against a cluster mean of roughly 6,500 kWh for the other eight materials. Flax maintains consistently low heating throughout the year, achieving stable group 'a' placement regardless of scenario. Glass wool's persistent group 'c'/'d' placement reflects its highest conductivity in the test set (30–50 mW/mK), which amplifies heat loss during cold periods.

Discussion

Loss of cooling leverage under warming

Cooling energy is statistically indistinguishable across all nine materials in four of the five future scenarios. The conductivity differences between tested materials (30–50 mW/mK for conventional versus 33–90 mW/mK for natural) are visible, but they are progressively overwhelmed by the magnitude of outdoor temperature forcing as scenarios intensify. When climate drives a 50–135% increase in cooling load from TMY to SSP5-2099, the material-level differences that once separated significance groups become negligible. This is consistent with Wang et al. (2022), who showed diminishing insulation returns on cooling performance in high-warming scenarios, though that study did not test convergence across material types.

The Tukey HSD test operates on daily energy distributions rather than annual totals. Under a given scenario, two materials with similar conductivities will produce daily cooling-load time series that are closely correlated. They track the same outdoor temperature forcing, differing only in the heat flux magnitude determined by their conductivity. As outdoor temperature forcing grows under warming, both the mean and the variance of daily cooling loads increase for all materials simultaneously. The between-material signal (the conductivity-driven difference in load) grows proportionally with warming, but the within-material daily variance (driven by extreme temperature events, solar gains, and occupancy fluctuations) also grows. When the within-material variance growth outpaces the between-material signal in high-forcing scenarios, the HSD test finds materials statistically indistinguishable even though absolute kWh differences persist.

The SSP1-2050 exception (CV = 9.41%) is instructive. It represents moderate near-term warming under a low-emissions pathway: elevated enough to shift load toward cooling, but not yet dominant enough to subsume all inter-material differences. That this differentiation vanishes at SSP5-2050, a warmer scenario at the same time horizon, confirms that convergence is driven by warming magnitude, not elapsed time.

Scenario-aware insulation specification

For practitioners specifying insulation in buildings expected to operate across mid-century, the SSP1-2050 result warrants attention: under mitigation-consistent pathways, material choice retains marginal relevance for cooling, but under high-emissions trajectories it becomes effectively irrelevant as a cooling-energy lever. In other words, the design leverage of insulation material type depends on the climate pathway the building will experience over its life, not just on present-day conditions.

This shift implies that specification decisions should become scenario-aware explicitly. In practice, this means distinguishing between buildings expected to operate primarily under low-warming, mitigation-consistent futures, where small cooling and heating differences across materials still justify careful selection—and those that are likely to face high-forcing futures, where climate pathway dominates, and cooling performance converges across conventional, bio-based, and recycled insulators.

What remains relevant in material choice

Glass wool's reversal requires emphasis. It goes from the lowest TMY total (101,094 kWh) to near-worst under sustained warming, with a +70% increase from TMY to SSP1-2099 versus +59% for EPS. The same conductivity that reduces winter heating losses in Austin's mild baseline climate amplifies summer cooling demand as outdoor temperature rises. This illustrates that even when cooling performance converges across most materials, specific products can still carry asymmetric risk profiles under warming.

Heating differentiation (CV 16–27%) persists across all scenarios (Figure 4), but its practical weight diminishes as heating contracts below 4% of total load by 2099 (Figure 3). Flax's consistent group 'a' performance (Figure 5) is mechanistically coherent: its specific heat capacity (1.6 J/g·°C) provides greater thermal buffering of diurnal swings, and its conductivity range (33 mW/mK) is competitive with EPS (29–41 mW/mK). For buildings designed now to operate through 2099, flax and XPS offer the most scenario-robust heating profiles. But as heating contracts below 4% of total load, even a group 'a' advantage is a small absolute saving; embodied carbon and material sustainability are the more consequential specification criteria for hot-climate contexts by 2099, as mentioned by Raja et al. (2023); Davey (2024).

Implications for codes and standards in hot-humid climates

Building codes calibrated against current climate may be structuring future performance risk for glass wool specifications in CZ2A, given its reversal from best to near-worst performer under warming. Prescriptive requirements that implicitly favor materials on the basis of present-climate heating benefits can unintentionally lock in higher cooling demand under future, hotter conditions.

As cooling-performance differences across insulation materials converge under SSP warming, code provisions and design guidelines for hot-humid, cooling-dominated climates should place less emphasis on fine-grained distinctions in insulation material for cooling optimization, and more emphasis on (i) robustness of heating behavior, (ii) embodied carbon and end-of-life impacts, and (iii) durability and moisture safety. Updating standards along these lines would better align envelope prescriptions with the trajectories of climate forcing that long-lived residential buildings in CZ2A and similar regions are likely to experience.

Generalizability and limitations

Several limitations bound these conclusions. The study examines a single building typology and climate zone (CZ2A); convergence dynamics will differ in heating-dominated climates where inter-material differences represent a larger load fraction. The exclusion of one rubber simulation introduces a gap at SSP1-2050. Lifecycle cost and embodied carbon are not quantified here, even though they are the specification criteria this paper argues should replace cooling optimization. Future work should integrate these dimensions directly. Extension to additional hot-humid cities, passive design typologies, and naturally ventilated configurations would strengthen the generalizability of the convergence finding.

While this study is limited to a single residential typology in a CZ2A hot-humid climate, the underlying mechanism driving cooling convergence—the growth of outdoor thermal forcing relative to material-level conductivity differences—should generalize to other strongly cooling-dominated contexts where future warming substantially increases cooling degree-hours. In heating-dominated or more balanced climates, by contrast, inter-material differences are likely to remain more consequential for both heating and cooling, and full convergence may not occur. Extending the same convergence-testing framework to additional climates and typologies is therefore a priority for identifying where insulation material remains a critical design variable and where climate forcing becomes dominant.

Conclusion

This paper evaluated whether insulation material type remains a meaningful cooling-energy design lever for a hot-humid CZ2A residential building under SSP-based future climates. Whole-building EnergyPlus simulations driven by SSP-morphed weather and analyzed with CV and Tukey HSD show that cooling-energy differences across nine conventional, bio-based, and recycled insulation materials converge into a single significance group in four of five future scenarios, while heating differentiation persists against a shrinking share of total load. In this context, climate pathway and urban heat island forcing, rather than insulation material identity at equivalent R-value, dominate future cooling outcomes. For long-lived buildings in similar cooling-dominated hot-humid climates, insulation specification should therefore be decoupled from cooling optimization and reoriented toward heating robustness, embodied carbon, and lifecycle criteria. Future work should apply the same convergence-testing framework across additional climates, building typologies, and combined operational–embodied performance metrics to map where insulation material choice remains decision-critical under climate change.

Data Availability Statement

The EnergyPlus simulation input files, climate morphing scripts, and extracted output data supporting the findings of this study are available from the corresponding author upon reasonable request.

Disclosure Statement

The authors declare no conflicts of interest.

Declaration of generative AI and AI-assisted technologies in the writing process

During the preparation of this work, the authors used Claude and Grammarly to improve readability and detect spelling/grammar mistakes. No graphics are generated through GenAI. After using this tool/service, the authors reviewed and edited the content as needed and take full responsibility for the content of the publication.

References

Aditya L, Mahlia TMI, Rismanchi B, Ng HM, Hasan MH, Metselaar HSC, Muraza O and Aditiya HB (2017) A review on insulation materials for energy conservation in buildings. *Renewable and Sustainable Energy Reviews* 73: 1352–1365. DOI:10.1016/j.rser.2017.02.034. URL https://www.sciencedirect.com/science/article/pii/S1364032117302484.

Austin Energy (2025) Open Data | City of Austin, Texas. URL https://data.austintexas.gov/login?return_to=%2Fstories%2Fs%2FAustin-Energy-Open-Data-Dashboard%2F82cz-8hvk.

Belcher S, Hacker J and Powell D (2005) Constructing design weather data for future climates. *Building Services Engineering Research & Technology* 26(1): 49–61. DOI: 10.1191/0143624405bt112oa. URL https://doi.org/10.1191/0143624405bt112oa.

Calama-González CM, León-Rodríguez and Suárez R (2023) Climate change mitigation: thermal comfort improvement in Mediterranean social dwellings through dynamic test cells modelling. *International Journal of Energy and*

Environmental Engineering 14(2): 121–134. DOI:10.1007/s40095-022-00498-1. URL https://doi.org/10.1007/s40095-022-00498-1.

Ciancio V, Salata F, Falasca S, Curci G, Golasi I and de Wilde P (2020) Energy demands of buildings in the framework of climate change: An investigation across Europe. *Sustainable Cities and Society* 60: 102213. DOI:10.1016/j.scs.2020.102213. URL https://www.sciencedirect.com/science/article/pii/S2210670720302006.

Cosentino L, Fernandes J and Mateus R (2023) A Review of Natural Bio-Based Insulation Materials. *Energies* 16(12): 4676. DOI:10.3390/en16124676. URL https://www.mdpi.com/1996-1073/16/12/4676.

Davey R (2024) Latest Developments in Sustainable Building Insulation Materials. URL https://www.azocleantech.com/article.aspx?ArticleID=1899. Section: Cleantech Article.

EIA (2022) Residential Energy Consumption Survey (RECS) - Energy Information Administration. URL https://www.eia.gov/consumption/residential/index.php.

Füchsl S, Rheude F and Röder H (2022) Life cycle assessment (LCA) of thermal insulation materials: A critical review. *Cleaner Materials* 5: 100119. DOI:10.1016/j.clema.2022.100119. URL https://www.sciencedirect.com/science/article/pii/S277239762200079X.

Grazieschi G, Asdrubali F and Thomas G (2021) Embodied energy and carbon of building insulating materials: A critical review. *Cleaner Environmental Systems* 2: 100032. DOI:10.1016/j.cesys.2021.100032. URL https://www.sciencedirect.com/science/article/pii/S2666789421000246.

Hosseini M, Javanroodi K and Nik VM (2022) High-resolution impact assessment of climate change on building energy performance considering extreme weather events and microclimate – Investigating variations in indoor thermal comfort and degree-days. *Sustainable Cities and Society* 78: 103634. DOI:10.1016/j.scs.2021.103634. URL https://www.sciencedirect.com/science/article/pii/S2210670721008970.

IEA (2022) Buildings - Energy System. URL https://www.iea.org/energy-system/buildings.

Invidiata A and Ghisi E (2016) Impact of climate change on heating and cooling energy demand in houses in Brazil. *Energy and Buildings* 130: 20–32. DOI:10.1016/j.enbuild.2016.07.067. URL https://www.sciencedirect.com/science/article/pii/S0378778816306776.

Jelle BP (2011) Traditional, state-of-the-art and future thermal building insulation materials and solutions – Properties, requirements and possibilities. *Energy and Buildings* 43(10): 2549–2563. DOI:10.1016/j.enbuild.2011.05.015. URL https://www.sciencedirect.com/science/article/pii/S0378778811002295.

Jentsch MF, James PAB, Bourikas L and Bahaj AS (2013) Transforming existing weather data for worldwide locations to enable energy and building performance simulation under future climates. *Renewable Energy* 55: 514–524. DOI:10.1016/j.renene.2012.12.049. URL https://www.sciencedirect.com/science/article/pii/S0960148113000232.

Kumar D, Alam M, Zou PXW, Sanjayan JG and Memon RA (2020) Comparative analysis of building insulation material properties and performance. *Renewable and Sustainable Energy Reviews* 131: 110038. DOI:10.1016/j.rser.2020.110038. URL https://www.sciencedirect.com/science/article/pii/S1364032120303294.

Nik VM (2016) Making energy simulation easier for future climate – Synthesizing typical and extreme weather data sets out of regional climate models (RCMs). *Applied Energy* 177: 204–226. DOI:10.1016/j.apenergy.2016.05.107. URL https://www.sciencedirect.com/science/article/pii/S0306261916307127.

Pittau F, Krause F, Lumia G and Habert G (2018) Fast-growing bio-based materials as an opportunity for storing carbon in exterior walls. *Building and Environment* 129: 117–129. DOI:10.1016/j.buildenv.2017.12.006. URL https://www.sciencedirect.com/science/article/pii/S0360132317305644.

Raja P, Murugan V, Ravichandran S, Behera L, Mensah RA, Mani S, Kasi A, Balasubramanian KBN, Sas G, Vahabi H and Das O (2023) A Review of Sustainable Bio-Based Insulation Materials for Energy-Efficient Buildings. *Macromolecular Materials and Engineering* 308(10): 2300086. DOI:10.1002/mame.202300086. URL https://onlinelibrary.wiley.com/doi/abs/10.1002/mame.202300086. _eprint: https://onlinelibrary.wiley.com/doi/pdf/10.1002/mame.202300086.

Rodrigues E, Fernandes MS and Carvalho D (2023) Future weather generator for building performance research: An open-source morphing tool and an application. *Building and Environment* 233: 110104. DOI:10.1016/j.buildenv.2023.110104. URL https://www.sciencedirect.com/science/article/pii/S0360132323001312.

Schiavoni S, DAlessandro F, Bianchi F and Asdrubali F (2016) Insulation materials for the building sector: A review and comparative analysis. *Renewable and Sustainable Energy Reviews* 62: 988–1011. DOI:10.1016/j.rser.2016.05.045. URL https://www.sciencedirect.com/science/article/pii/S1364032116301551.

Schulte M, Lewandowski I, Pude R and Wagner M (2021) Comparative life cycle assessment of bio-based insulation materials: Environmental and economic performances. *GCB Bioenergy* 13(6): 979–998. DOI:10.1111/gcbb.12825. URL https://onlinelibrary.wiley.com/doi/abs/10.1111/gcbb.12825. _eprint: https://onlinelibrary.wiley.com/doi/pdf/10.1111/gcbb.12825.

UT-City Climate CoLab (2024) Austin Future Climate: Climate Projections For the City of Austin. URL https://texuslab.org/colab.

Wang R, Lu S, Zhai X and Feng W (2022) The energy performance and passive survivability of high thermal insulation buildings in future climate scenarios. *Building Simulation* 15(7): 1209–1225. DOI:10.1007/s12273-021-0818-3. URL https://doi.org/10.1007/s12273-021-0818-3.